Photoneutron cross sections for $^{118-124}$Sn and the γ-ray strength function method

H. Utsunomiya,[1] S. Goriely,[2] M. Kamata,[1] H. Akimune,[1] T. Kondo,[1] O. Itoh,[1] C. Iwamoto,[1] T. Yamagata,[1] H. Toyokawa,[3] Y.-W. Lui,[4] H. Harada,[5] F. Kitatani,[5] S. Goko,[6] S. Hilaire,[7] and A. J. Koning[8]

[1]*Department of Physics, Konan University, Okamoto 8-9-1, Higashinada, Kobe 658-8501, Japan*
[2]*Institut d'Astronomie et d'Astrophysique, Université Libre de Bruxelles, Campus de la Plaine, CP-226, 1050 Brussels, Belgium*
[3]*National Institute of Advanced Industrial Science and Technology, Tsukuba 305-8568, Japan*
[4]*Cyclotron Institute, Texas A&M University, College Station, Texas 77843, USA*
[5]*Japan Atomic Energy Agency, Tokai-mura, Naka, Ibaraki 319-1195, Japan*
[6]*Faculty of Engineering Hokkaido University, Sapporo 060-8628, Japan*
[7]*CEA, DAM, DIF, F-91297 Arpajon, France*
[8]*Nuclear Research and Consultancy Group, P.O. Box 25, NL-1755 ZG Petten, The Netherlands*

(Received 19 August 2011; published 22 November 2011)

Photoneutron cross sections were measured for ^{118}Sn, ^{119}Sn, ^{120}Sn, ^{122}Sn, and ^{124}Sn near neutron threshold with quasi-monochromatic laser-Compton scattering γ rays. A systematic analysis of the present photoneutron data and existing neutron-capture data is made using the γ-ray strength function on the basis of the HFB + QRPA model of $E1$ strength supplemented with a pygmy dipole resonance, which was deduced from a previous study on ^{116}Sn and ^{117}Sn. Radiative neutron capture cross sections for two radioactive nuclei, ^{121}Sn and ^{123}Sn, are deduced through the γ-ray strength function method.

DOI: 10.1103/PhysRevC.84.055805 PACS number(s): 25.20.Lj, 21.10.Pc, 24.30.Gd, 27.60.+j

I. INTRODUCTION

The γ-ray strength function (γSF) is a nuclear statistical quantity that governs electromagnetic processes in radiative neutron captures and photoneutron emissions. The leading term of the γSF is the $E1$ strength which extends from the peak region of the giant dipole resonance (GDR) to the tail region above and below neutron threshold [1,2]. Besides the GDR, an extra strength known as pygmy resonance (PR) is expected to emerge at low energy around the neutron threshold. The PR is interpreted as a new excitation mode related to the dipole oscillation of a neutron skin against a core nuclei with $N = Z$ [3] though there may be a different picture like low energy $E1$ strength that fails to participate in the GDR excitation. Besides the physics picture, the degree of collectivity involved in the excitation of PR is currently controversial [4–7].

The γSF in tin isotopes has been investigated experimentally with the Oslo method using (^{3}He, ^{3}He'γ), (^{3}He, $\alpha'\gamma$) and (α, $\alpha'\gamma$) reactions for $^{116-122}$Sn [8–10], while PR has been investigated in the nuclear resonance fluorescence experiment for ^{116,124}Sn [11] and with the (α, $\alpha'\gamma$) coincidence technique for ^{124}Sn [12]. The γ-ray detections probe the γSF and PR below the neutron threshold; the former measurements with NaI(Tl) detectors probe the γSF and the nuclear level density in an entangled way, while the latter measurements with Ge detectors favors to identify strong $E1$ transitions rather than weak $M1$ transitions that are possibly fragmented. Furthermore, PR in ^{130,132}Sn above neutron threshold was investigated in Coulomb dissociation [13]. A threshold-free high-resolution inelastic proton scattering experiment was recently proposed to investigate an $E1$ strength distribution in ^{120}Sn [14].

The role of the γ-ray strength in nuclear astrophysics and nuclear engineering was discussed in Refs. [1,2]. Since the (γ,n) and (n,γ) reaction cross section are interconnected through the γSF in the Hauser-Feshbach model, an indirect method called the γ-ray strength function method was devised for constraining radiative neutron capture cross sections for unstable nuclei [2] and applied to ^{93,96}Zr and ^{107}Pd [2,15].

Recently, we measured photoneutron cross sections for ^{116,117}Sn near neutron threshold and showed that the Skyrme Hartree-Fock-Bogoliubov (HFB) plus quasiparticle random-phase approximation (QRPA) model of $E1$ strength supplemented with a pygmy dipole resonance reproduce satisfactorily both (γ,n) cross sections for ^{116,117}Sn and (n,γ) cross sections for ^{116}Sn [1]. We recently extended our photoneutron cross section measurement to five tin isotopes (^{118,119,121,122,124}Sn) for a systematic study, excluding three isotopes (^{112,114,115}Sn) with low natural abundances (0.34–0.97%). Such a systematic measurement allows us to apply the so-called γSF method. In this application, the following three steps are depicted in Fig. 1: 1) measurements of (γ,n) cross sections for stable tin isotopes (left arrows); 2) investigation, extrapolation, and justification of the γSF which interconnects (γ,n) and (n,γ) cross sections (right arrows); and 3) prediction of (n,γ) cross sections within the statistical model calculation for the radioactive ^{121}Sn and ^{123}Sn with half-lives of 27 h and 129 d, respectively. Radiative neutron capture cross sections for ^{121}Sn and ^{123}Sn constitute nuclear inputs of particular interest to the s-process nucleosynthesis.

The present measurement provides photoneutron cross sections for ^{122}Sn for the first time, for ^{119}Sn near threshold including previously unexplored energies below 9.0 MeV, and for ^{118,124}Sn for which the Livermore [16] and Saclay [17] data show large discrepancies. The new measurements are described in Sec. II and compared with previous data as well as theoretical calculations in Sec. III.

FIG. 1. (Color online) The chart of nuclei depicting an application of the γ-ray strength function method to tin isotopes. Photoneutron cross sections measured in the present experiment are shown by left arrows. Radiative neutron capture cross sections used for constraining the γSF are show by right arrows. Photoneutron cross sections for two radioactive nuclei, ^{121}Sn and ^{123}Sn, are deduced with the γ-ray strength function method.

II. PHOTONEUTRON CROSS SECTION MEASUREMENTS

The experiment was performed with quasi-monochromatic laser-Compton scattering (LCS) γ rays at the National Institute of Advanced Industrial Science and Technology (Japan). The LCS γ rays were produced with a high-intensity Nd:YVO_4 Q-switch laser that generate 1064-nm photons at 40 W and 532-nm photons at 24 W with a frequency-doubler module in the energy range from 6.78 MeV to 13.00 MeV (energies are quoted as the maximum energies of the LCS γ-ray beams). Enriched materials of ^{118}Sn (98.50%, 1500 mg metal), ^{119}Sn (93.00%, 1023 mg metal), ^{120}Sn (98.80%, 1492 mg metal), ^{122}Sn (94.60%, 1200 mg metal powder), and ^{124}Sn (97.90%, 1994 mg metal) were pressed/shaped into targets of 8 mm diameter and 2.8–5.0 mm lengths. A high-efficiency 4π neutron detector composed of triple rings of 20 ^{3}He proportional counters altogether embedded in a polyethylene moderator was used for neutron detection. Neutron events from major isotopic impurities, ^{118}Sn (6.4%) and ^{120}Sn (3.02%) included in the ^{119}Sn and ^{122}Sn target materials, respectively, were directly determined and subtracted in the present measurements. Contributions from impurities included in the ^{118,120,124}Sn materials with the high enrichments were neglected. Measurements below neutron threshold were carried out for ^{118}Sn at 9.0 MeV, ^{120}Sn at 9.0 MeV, ^{122}Sn at 8.50 MeV, and ^{124}Sn at 8.25 MeV. No significant neutron events were observed. The number of the LCS γ rays incident on the targets was determined from pileup- and single-photon spectra measured with a 8 in. diameter $\times$12 in. length NaI(Tl) detector. The LCS γ-ray beam was measured with the high-resolution high-energy photon spectrometer (HHS) [19] at a reduced laser power to determine the energy distributions of the LCS γ-ray beam by means of the unfolding technique [20,21]. The measurement was repeatedly made typically every hour, intervening the photoneutron measurements with the full laser power. The energy spread of the beam was 6%–13% in the full width at half-maximum. Note, however, that the LCS γ rays in the energy interval between the neutron threshold and the maximum beam energy are responsible for inducing photoneutron emissions. The energy interval is smaller than the energy spread of the beam in measurements immediately above the neutron threshold. More details of the experimental procedure are found in Refs. [1,22].

Photoneutron cross sections were deduced at the average γ-ray energies with the χ^2-fitting method for ^{118,119,120,122}Sn and the Taylor expansion method for ^{124}Sn [1]. The two data-reduction methods are known to work consistently in deducing photoneutron cross sections [1]. The systematic uncertainty for the cross section is $\pm$4.4% which represents a quadratic sum of uncertainties of the neutron detection efficiency (3.2%) and the number of incident γ rays (3%). The final cross sections are shown in Figs. 2–6 and compared with previous measurements or evaluations. As can be seen, quite some discrepancies are found close to the neutron threshold, in particular for ^{119}Sn and ^{122}Sn. Note that Varlamov *et al.* [18] evaluated photoneutron cross sections for Sn isotopes by analyzing experimental data taken with bremsstrahlung and quasi-monochromatic photon

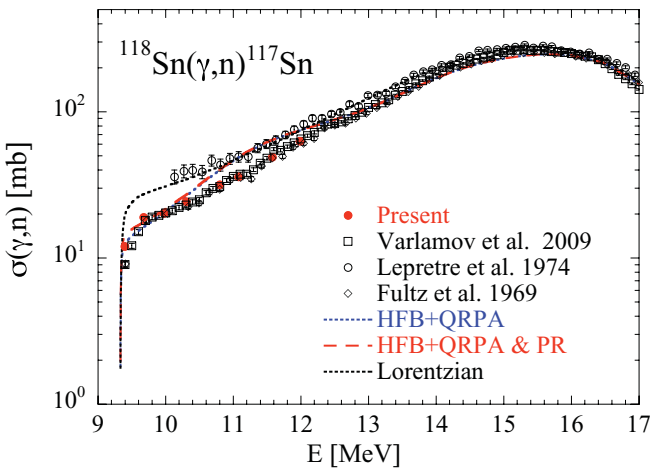

FIG. 2. (Color online) ^{118}Sn(γ,n)^{117}Sn photoneutron cross section. The full dots correspond to our new measurements and the other symbols to the former photodata [16,17] and the evaluated cross sections [18]. The theoretical cross sections considered in this study (see text) are also shown.

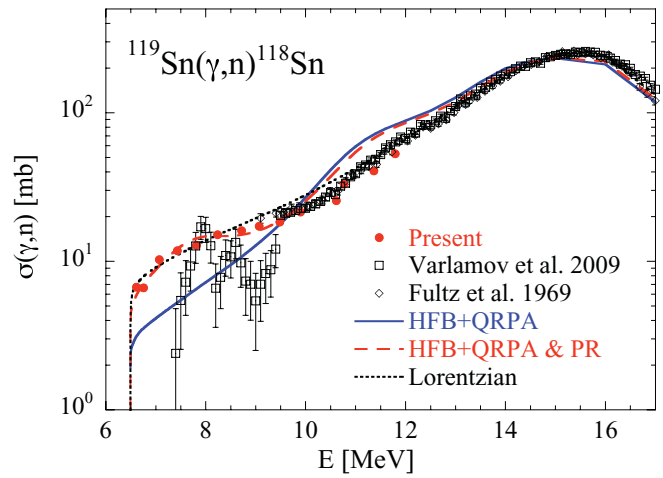

FIG. 3. (Color online) Same as Fig. 2 for the ^{119}Sn(γ,n)^{118}Sn photoneutron cross section.

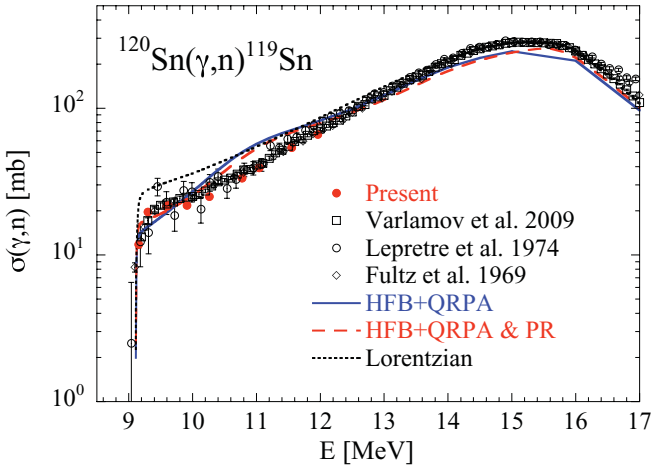

FIG. 4. (Color online) Same as Fig. 2 for the ^{120}Sn(γ,n)^{119}Sn photoneutron cross section.

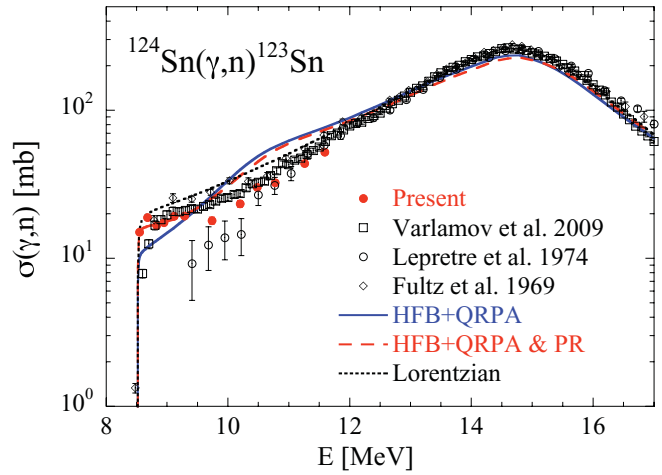

FIG. 6. (Color online) Same as Fig. 2 for the ^{124}Sn(γ,n)^{123}Sn photoneutron cross section.

beams produced in the positron annihilation in flight. The cross sections are further analyzed below.

III. THEORETICAL INTERPRETATION

Theoretically, as done in our study on the photoemission of ^{116,117}Sn [1], the experimental data have been analyzed on the basis of the TALYS reaction code [23] and different γ-ray strength functions, namely the Lorentzian model [24] and the Skyrme HFB plus QRPA model [25]. As seen in Figs. 2–6, cross sections around the neutron threshold are rather overestimated by the Lorentzian model and underestimated by the HFB + QRPA model (note that a shift of about 0.2–0.5 MeV has been applied to the HFB + QRPA strength to normalize the cross section on the experimentally measured centroid energy). This underestimation was already observed for the ^{116,117}Sn(γ,n) reactions and interpreted as a lack of $E1$ strength [1], where it was shown that a simple increase of the $E1$ strength through an additional PR could solve the discrepancies. This is shown in Figs. 2–6 by the HFB + QRPA and PR calculation which on top of the HFB + QRPA $E1$ strength also includes a $E1$ PR characterized by a centroid energy of about 8–8.5 MeV (8.5 MeV for ^{118}Sn and 8 MeV for the heavier isotopes), a width of 2 MeV, and peak strength corresponding to a cross section of 7 mb. The resulting model is identical to the one applied in Ref. [1] to ^{116,117}Sn. In the present cases, it can be seen in Figs. 2–6, that the agreement around the neutron threshold is rather satisfactory. Note that the HFB + QRPA systematically predicts some extra strength around 11 MeV that is not observed in the photoemission cross sections measured here. This extra PR strength is partially due to the effective interaction considered, but also to some missing effect such as the quasiparticle-phonon coupling. Such recent calculations have indeed confirmed that this latter effect can shift the PR to lower excitation energies by about 2 MeV [26,27]. However, this energy region is not of particular relevance in our present study since we essentially focus here on the tail of the GDR. Figs. 2–6, in addition of Figs. 3 and 5 of Ref. [1] show that all the measured Sn photoemission cross sections in the vicinity of the neutron threshold can be consistently explained by the HFB + QRPA model provided an extra E1 PR is included.

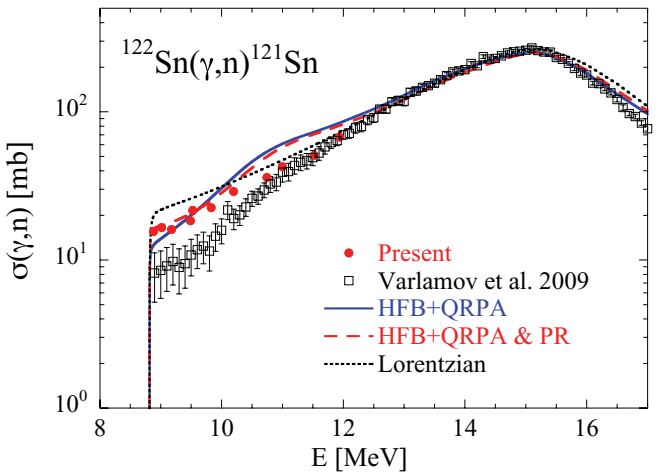

FIG. 5. (Color online) Same as Fig. 2 for the ^{122}Sn(γ,n)^{121}Sn photoneutron cross section.

To further confirm the presence of the low-lying PR around 8 MeV, like in our previous study [1], we now consider the inverse radiative neutron captures for keV neutron energies which are known experimentally and sensitive to the γ strength below the neutron threshold. Note that we assume here, as classically done, that the de-excitation electromagnetic strength is directly related to the photoabsorption strength function, i.e., $f(E_\gamma) \downarrow = f(E_\gamma) \uparrow$, no T-dependence being introduced in the present study. A coherent comparison of the neutron capture data with the Lorentzian and HFB + QRPA (including a PR) is shown in Figs. 7–9 for $^{117-119}$Sn(n,γ)$^{118-120}$Sn, where exactly the same $E1$ strengths as used in Figs. 2–4 have been used. For ^{116}Sn, see Fig. 4 of Ref. [1]. Although in cases where the neutron separation energy is rather high (e.g., Fig. 7), the PR has no major influence, the HFB + QRPA strength clearly gives reasonable predictions and is improved when including the PR contribution. In contrast,

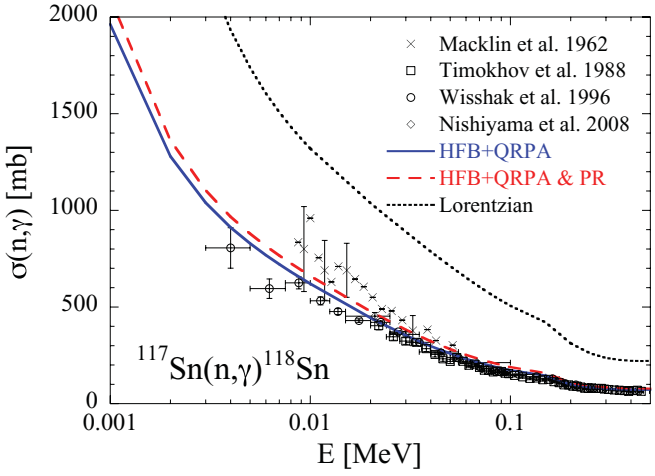

FIG. 7. (Color online) ^{117}Sn$(n,\gamma)^{118}$Sn cross section obtained with the HFB + QRPA, HFB + QRPA and PR and Lorentzian $E1$ strengths (see Fig. 2) and compared with experimental data [28–31].

the Lorentzian model systematically overestimates the cross section, so that the Lorentzian model should not be applied to the calculation of radiative neutron captures, as also concluded in our previous studies (see, e.g., [1]). Note that the radiative neutron capture cross section is also relatively sensitive to the nuclear level density. The model adopted here is the HFB plus combinatorial model [32]. Experimental data exists to constrain the level density in $^{118-120}$Sn around the neutron binding energy, namely the s-wave resonance spacing [24], so that the uncertainties affecting the level density predictions are not found to change the above-mentioned conclusion (the impact on the radiative neutron capture cross section is in these cases typically around 30%).

For all these reasons, the present data strongly suggest the existence of an additional low-lying strength in agreement with the nuclear resonance fluorescence data [11] and the recent measurements of the Oslo group [9,10,33]. In the latter case, the radiative strength function was deduced from the analysis of the (^{3}He,^{3}He$'\gamma$) reaction and found to be compatible with the presence of a PR around 8 MeV with an integrated strength

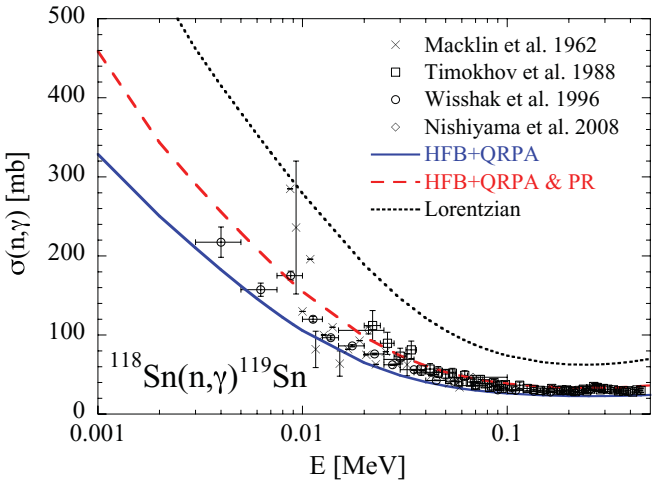

FIG. 8. (Color online) Same as Fig. 7 for ^{118}Sn$(n,\gamma)^{119}$Sn.

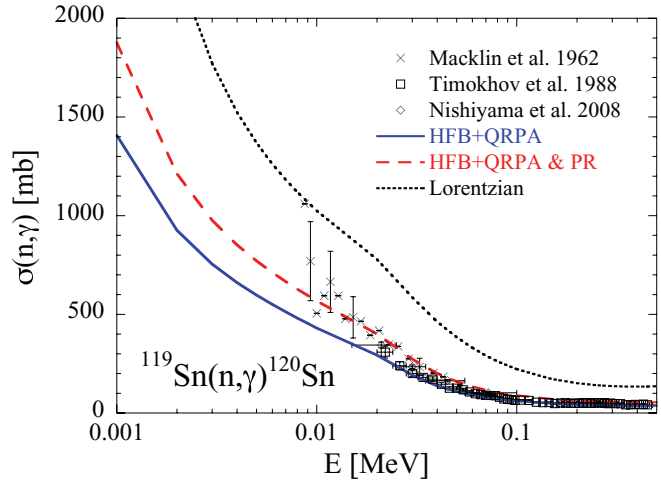

FIG. 9. (Color online) Same as Fig. 7 for ^{119}Sn$(n,\gamma)^{120}$Sn.

corresponding to 1.7% of the classical Thomas-Reiche-Kuhn sum rule. The HFB + QRPA strength (with and without the inclusion of the PR) is compared in Fig. 10 with Oslo experimental data [9,10] as well as the present photoneutron data and those of Ref. [18] for ^{118,119,122}Sn (note that the strength function is extracted from the photo cross section by the approximate relation $f_\gamma = \sigma/E$, although this relation is only valid for total photoabsorption cross section). Here again, the data is clearly in favor of some extra γ-ray strength at energies around 6–8 MeV.

The presence of this extra PR strength is an important theoretical issue. Recent models have been developed and could potentially provide some explanation for this PR. It concerns the self-consistent variant of the microscopic extended theory of finite Fermi systems, which, in addition to the QRPA approach, takes the single-particle continuum and phonon coupling into account [26,27]. These calculations confirm the need to take into account more complex configurations than those included in the standard QRPA, namely the $1p1h \otimes$ phonon or two quasiparticles $\otimes$ phonon configurations. Such calculations were performed for the ^{100,124,132,150}Sn isotopes on the basis of the SLy4 Skyrme interaction [26,27] and found an increase of the strength at low energies, typically around 7–9 MeV. In particular, in ^{124}Sn, the contribution due to the phonon coupling increases the $E1$ strength around 8 MeV by about a factor of 5. Similar results for the Sn isotopes were also obtained within the relativistic QRPA model [34] which also predicts systematically an extra $E1$ strength around 8 MeV. More work in this direction could shed light on the systematics of PR energy and strengths.

On the basis of the present analysis, the radiative neutron capture by the unstable ^{121}Sn and ^{123}Sn is now estimated. For both reactions, the γ-ray strength functions of the compound systems, ^{122}Sn and ^{124}Sn, respectively, are strongly constrained around the neutron threshold by our new experiments (see Figs 5 and 6). The rather satisfactory agreement between our systematics of neutron captures (see Figs. 7–9) also gives some confidence on the corresponding predictions for ^{121}Sn and ^{123}Sn neutron captures. However, nuclear level densities are in these cases not constrained by s-wave spacings at the neutron

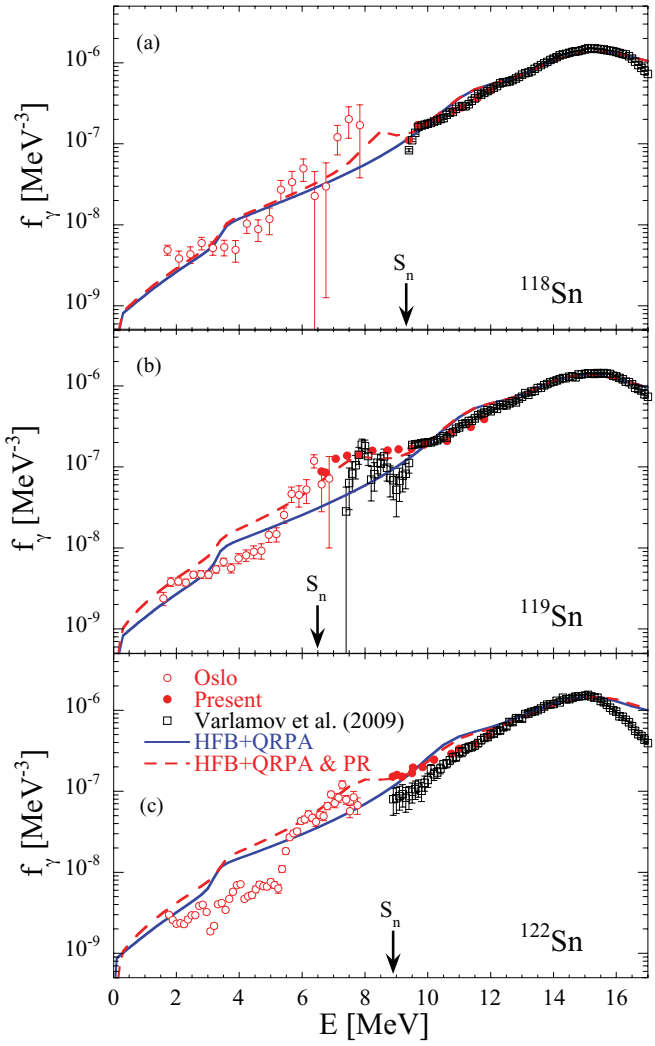

FIG. 10. (Color online) Comparison between the HFB + QRPA strength (with and without the inclusion of the PR) and the experimental data of the Oslo group [9,10], from photodata [18] as well as the present photoemission data, for ^{118}Sn (a), ^{119}Sn (b), and ^{122}Sn (c).

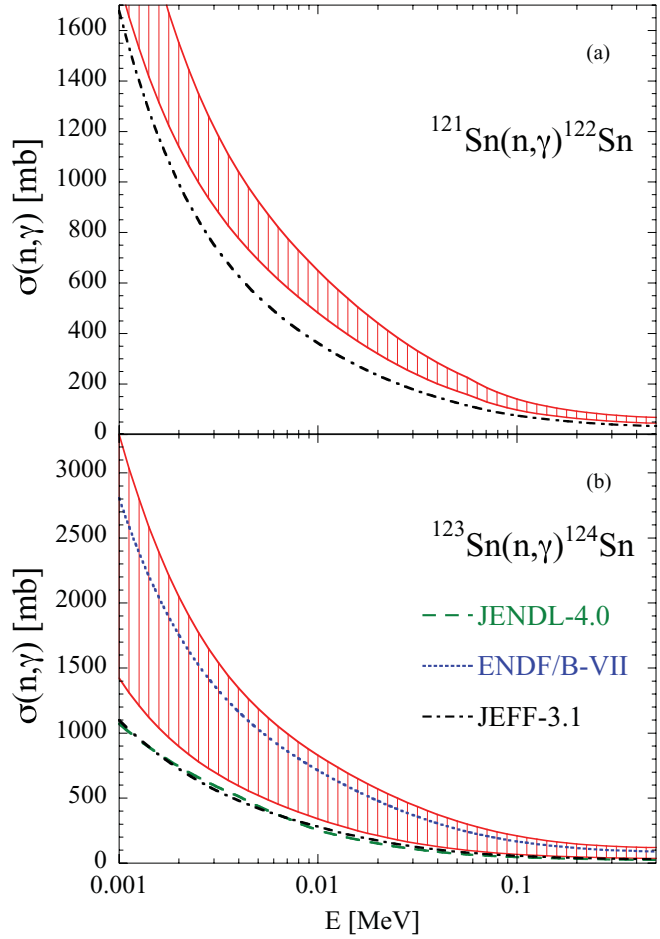

FIG. 11. (Color online) ^{121}Sn$(n,\gamma)^{122}$Sn (a) and ^{123}Sn$(n,\gamma)^{124}$Sn (b) cross sections obtained with the HFB + QRPA and PR $E1$ strengths (see Fig. 5 and 6). The uncertainties are associated with the use of different nuclear level density models [35]. The dashed, dotted, and dash-dot curves correspond to the Japanese JENDL-4.0, American ENDF/B-VII, and European JEFF-3.1 evaluations, respectively [36], whenever available.

separation energy, but only by low-lying level schemes. To estimate the uncertainties associated with unknown nuclear level densities, we consider the models described in Ref. [35]. Such models affect the cross section predictions at a few tens of keV energies by typically 30% for ^{121}Sn$(n,\gamma)^{122}$Sn and by a factor of 2 for ^{123}Sn$(n,\gamma)^{124}$Sn, as shown in Fig. 11. The newly determined cross sections are also compared in Fig. 11 with the predictions found in the widely used JENDL, ENDF/B, and JEFF libraries [36]. Only the ENDF/B estimate of the ^{123}Sn neutron capture cross section is found compatible with our present study.

The present photoneutron cross section measurement alone cannot distinguish the multipolarity of extra strengths. Previously the presence of giant $M1$ resonance was assumed in zirconium isotopes [2,37], being supported by the inelastic proton scattering experiment [38], but not by the photon scattering experiments [39,40]. The multipole decomposition of extra strengths into $E1$ and $M1$ is an urgent experimental issue. The nuclear resonance fluorescence experiment with linearly polarized photons may provide useful information below neutron threshold [41]. Furthermore, there emerge new experimental activities to address this issue, including asymmetry measurements of photoneutrons for deuteron [42] and ^{208,207}Pb [43] and new-generation experiments of inelastic proton scattering around zero degrees for ^{120}Sn [14] and ^{208}Pb [44], and $N = 50$ isotones (^{88}Sr, ^{90}Zr, ^{92}Mo) [45].

IV. CONCLUSION

We have completed a systematic measurement of photoneutron cross sections for stable tin isotopes with $A = 116$–124 using quasi-monochromatic laser-Compton scattering γ-ray beams. In the context of an application of the γSF method, we have investigated the γ-ray strength function that interconnects (γ,n) and (n,γ) cross sections in the statistical reaction model and reasonably well reproduced the photoneutron and radiative neutron-capture cross sections for tin isotopes with

the HFB + QRPA model of $E1$ strength supplemented with a pygmy dipole resonance. The PR was parametrized by a centroid energy of 8.0–8.5 MeV and an integrated strength about 1% (a width of 2 MeV and a peak cross section of 7 mb) of the Thomas-Reiche-Khun sum rule. The present γSF and PR obtained with the γSF method are qualitatively in good agreement with those obtained with the Oslo method [9,10]. Radiative neutron capture cross sections for ^{121}Sn and ^{123}Sn with the half-lives of 27 h and 129 d, respectively, were deduced with the γSF method. The associated uncertainty originating from the nuclear level density is as large as 30% for ^{121}Sn and a factor of 2 for ^{123}Sn. Finally, we note a shortcoming of the HFB + QRPA model of E1 strength that slightly overestimates photoneutron cross sections for the tin isotopes in the region of 10–12 MeV. This shortcoming of the γ-ray strength function only affects the (γ,n) cross sections, but has no impact on the (n,γ) cross sections.

ACKNOWLEDGMENTS

We thank M. Igashira of the Tokyo Institute of Technology for lending us the enriched ^{124}Sn material for the present measurement. This work is supported by the Japan Private School Promotion Foundation and the Konan-ULB bilateral project. S.G. acknowledges the financial support of the "Actions de recherche concertées (ARC)" from the "Communauté française de Belgique" and from the F.N.R.S.

[1] H. Utsunomiya *et al.*, Phys. Rev C **80**, 055806 (2009).
[2] H. Utsunomiya *et al.*, Phys. Rev. C **82**, 064610 (2010).
[3] N. Parr *et al.*, Rep. Prog. Phys. **70**, 691 (2007).
[4] Y. Suzuki *et al.*, Prog. Theor. Phys. **83**, 180 (1990).
[5] D. Vretenar, N. Paar, P. Ring, and G. A. Lalazissis, Phys. Rev. C **63**, 047301 (2001).
[6] D. Sarchi *et al.*, Phys. Lett. B **601**, 27 (2004).
[7] G. Co, V. DeDonno, C. Maieron, M. Anguiano, and A. M. Lallena, Phys. Rev. C **80**, 014308 (2009).
[8] U. Agvaanluvsan *et al.*, Phys. Rev. Lett. **102**, 162504 (2009).
[9] H. K. Toft *et al.*, Phys. Rev. C **81**, 064311 (2010).
[10] H. K. Toft *et al.*, Phys. Rev. C **83**, 044320 (2011).
[11] K. Govaert *et al.*, Phys. Rev. C **57**, 2229 (1998).
[12] J. Endres *et al.*, Phys. Rev. Lett. **105**, 212503 (2010).
[13] P. Adrich *et al.*, Phys. Rev. Lett. **95**, 132501 (2005).
[14] A. M. Heilmann, Master Thesis, TU-Darmstadt (November 2009); Experiment ID E316 approved at RCNP, Osaka University; [http://www.rcnp.osaka-u.ac.jp/Divisions/plan/b-pac/ex_appro/index.html].
[15] H. Utsunomiya *et al.*, Phys. Rev C **81**, 035801 (2010).
[16] S. C. Fultz, B. L. Berman, J. T. Caldwell, R. L. Bramblett, and M. A. Kelly, Phys. Rev. **186**, 1255 (1969).
[17] A. Lepretre, H. Beil, R. Bergere, P. Carlos, A. Deminiac, and V. Veyssiere, Nucl. Phys. A **219**, 39 (1974).
[18] V. V. Varlamov, B. S. Ishkhanov, V. N. Orlin, and V. A. Tchetvertkova, Moscow State University Institute of Nuclear Physics Report No. 2009, (2009), p. 3/847 (see also EXFOR library at [http://www-nds.iaea.or.at/exfor]).
[19] H. Harada and Y. Sigetome, J. Nucl. Sci. Technol. **32**, 1189 (1995).
[20] H. Harada *et al.*, Nucl. Instrum. Methods Phys. Res. A **554**, 306 (2005).
[21] H. Utsunomiya *et al.*, Nucl. Instrum. Methods Phys. Res. A **548**, 455 (2005).
[22] A. Makinaga *et al.*, Phys. Rev C **79**, 025801 (2009).
[23] A. J. Koning, S. Hilaire, and M. Duijvestijn, in *Nuclear Data for Science and Technology*, edited by O. Bersillon *et al.* (EDP Sciences, 2008), p. 211.
[24] R. Capote, M. Herman, P. Oblozinsky *et al.*, Nucl. Data Sheets **110**, 3107 (2009).
[25] S. Goriely, E. Khan, and M. Samyn, Nucl. Phys. A **739**, 331 (2004).
[26] A. Avdeyenkova, S. Goriely, S. Kamerdzhiev, and G. Tertychny, *Capture Gamma Ray Spectroscopy and Related Topics* [AIP series **1090**, 149 (2009)].
[27] A. Avdeenkov, S. Goriely, S. Kamerdzhiev, and S. Krewald, Phys. Rev. C **83**, 064316 (2011).
[28] R. L. Macklin, T. Inada, and J. H. Gibbons, Nature (London) **194**, 1272 (1962).
[29] V. M. Timokhov *et al.*, Yad. Fiz. **50**, 609 (1988).
[30] K. Wisshak *et al.*, Phys. Rev. C **54**, 1451 (1996).
[31] J. Nishiyama, M. Igashira, T. Ohsaki, G. N. Kim, W. C. Chung, and T. I. Ro, J. Nucl. Sci. Technol. **45**, 352 (2008).
[32] S. Goriely, S. Hilaire, and A. J. Koning, Phys. Rev. C **78**, 064307 (2008).
[33] U. Agvaanluvsan *et al.*, Phys. Rev. Lett. **102**, 162504 (2009).
[34] I. Daoutidis and S. Goriely, Phys. Rev. C **84**, 027301 (2011).
[35] A. J. Koning, S. Hilaire, and S. Goriely, Nucl. Phys. A **810**, 13 (2008).
[36] Evaluated Nuclear Data Files, 2011, [http://www-nds.iaea.or.at/exfor/endf.htm].
[37] H. Utsunomiya *et al.*, Phys. Rev. Lett. **100**, 162502 (2008).
[38] G. M. Crawly *et al.*, Phys. Rev. C **26**, 87 (1982).
[39] R. M. Laszewski, R. Alarcon, and S. D. Hoblit, Phys. Rev. Lett. **59**, 431 (1987).
[40] R. Schwengner *et al.*, Phys. Rev. C **78**, 064314 (2008).
[41] A. P. Tonchev *et al.*, Phys. Rev. Lett. **104**, 072501 (2010).
[42] C. Iwamoto *et al.*, AIP Conf. Proc. **1238**, 301 (2010).
[43] T. Kondo, AIP Conf. Proc. **1238**, 231 (2010).
[44] A. Tamii *et al.*, Phys. Rev. Lett. **107**, 062502 (2011).
[45] C. Iwamoto, Experiment ID E326 approved at RCNP, Osaka University; [http://www.rcnp.osaka-u.ac.jp/Divisions/plan/b-pac/ex_appro/index.html].